THE BELL SYSTEM TECHNICAL JOURNAL
Vol. 51, No. 3, March, 1972
Printed in U.S.A.

The Identification of Modal Resonances in Ferrite Loaded Waveguide Y-Junctions and Their Adjustment for Circulation

By B. OWEN

(Manuscript received September 24, 1971)

This paper reports on extensive eigenvalue measurements made on an X-band waveguide Y-junction containing different ferrite geometries. The frequency dependence of the eigenvalues is used to identify the principal field modes involved, to examine their sensitivities to various junction parameters, and to arrange their correct displacement for circulation. The knowledge gained from these measurements is used to explain the mode of operation of the partial height ferrite Y-junction circulator, and to introduce other novel configurations.

I. INTRODUCTION

The waveguide Y-junction circulator was first introduced by H. N. Chait and T. R. Curry in 1959.[1] During the past ten years it has become a widely used device. Surprisingly, its exact mode of operation has never been clearly understood. Numerous analyses and theories have been proposed for the device, but none has proven entirely satisfactory.

A fundamental theory for the circulator in terms of its external properties was first presented by B. A. Auld in 1959.[2] He showed that the junction scattering matrix was characterized by three eigenvalues which had to be phase displaced by 120 degrees for circulation. The theory, however, did not show how this displacement was to be achieved since this required a more detailed field theory analysis of the junction involved.

Such an analysis for the stripline circulator was first carried out by H. Bosma in 1962.[3] Based on Bosma's results, C. E. Fay and R. L. Comstock in 1965 presented a simplified "two resonant mode" theory for the stripline device together with experimental evidence of the validity of their approximations.[4] This theory was later improved by W. H. von Aulock and Fay in 1968.[5] For lack of a suitable alternative,

the "two resonant mode" theory also became the accepted explanation for the waveguide circulator. The theory stated that circulation occurred in the region between two diametrically determined resonances which were split apart by the applied field. The ferrite saturation magnetization had to be large enough to provide adequate splitting and low enough to avoid low field loss; and the ferrite dimensions had to be suitable for resonance at the desired frequency. A quarterwave transformer also had to be included for broadband matching.

While this explanation seemed satisfactory for the stripline device, it was inadequate for the waveguide case. Attempts to broadband models designed on this basis were rarely successful, and the development was always completed in a cut-and-try manner. An important outcome of these empirical adjustments, however, was the discovery of the partial height ferrite circulator. This seemed capable of larger bandwidths than its full height ferrite counterpart, and it rapidly became established as a standard design. In fact, most broadband devices in use today are of this nature. The discrepancies between the "two resonant mode" theory and the mode of operation of the partial height ferrite device were never clearly explained.

Field theory analyses for the waveguide circulator itself were carried out by J. B. Davies in 1962 and H. J. Butterweck in 1963.[6,7] Davies' analysis provided a solution for the Y-junction boundary value problem by matching the dominant mode fields in the connecting waveguides to a summation of fields due to modes within the junction. The mathematical complexity of the analysis, however, obscured any simplified explanation for circulation. Nevertheless, it did provide a numerical means of circulator synthesis. The only restriction imposed was that the field variation in the direction parallel to the symmetry axis be zero. This limited the analysis to junctions with full height components only. It excluded the partial height ferrite circulators designed since 1959, and narrow bandwidths were at first anticipated. However, in 1965 Davies extended the technique to junctions with more complex full height elements, and predicted much larger bandwidths.[8] The ferrite had a small conducting pin along its axis, and was surrounded by a dielectric sleeve. These predictions were confirmed by C. G. Parsonson, et al., in 1968, and since then near full waveguide bandwidth devices of this nature have been reported by J. B. Castillo and L. E. Davis.[9,10]

In this paper, a useful technique for determining the mode of operation of waveguide circulators is described. It involves a measuring set, operating at X-band, that is capable of displaying the junction eigen-

values as functions of frequency. The phase-frequency responses of the eigenvalues are used to identify the principal field modes involved in each case, and to examine their sensitivities to various junction parameters. The experimental results taken provide an explanation for various types of circulators, and also introduce other novel configurations.

II. THEORY

2.1 *Eigenvalue Analysis*

The scattering matrix $[S]$ of a 3-port junction is given by:

$$[S] = \begin{bmatrix} S_{11} & S_{12} & S_{13} \\ S_{21} & S_{22} & S_{23} \\ S_{31} & S_{32} & S_{33} \end{bmatrix}, \tag{1}$$

where S_{pp} is the reflection coefficient at port p, and S_{pq} is the transmission coefficient from port q to port p. If the junction is symmetrical then:

$$[S] = \begin{bmatrix} S_{11} & S_{12} & S_{13} \\ S_{13} & S_{11} & S_{12} \\ S_{12} & S_{13} & S_{11} \end{bmatrix}, \tag{2}$$

where

$$\begin{aligned} S_{11} &= S_{22} = S_{33} , \\ S_{12} &= S_{23} = S_{31} , \\ S_{13} &= S_{21} = S_{32} . \end{aligned} \tag{3}$$

The scattering matrix of the symmetrical junction is characterized by three eigensolutions:

$$[S][x]_i = \phi_i[x]_i ; \qquad i = 1, 2, 3 \tag{4}$$

where $[x]_i$ are the eigenvectors and ϕ_i are the eigenvalues. A vector in this case represents three signals applied simultaneously at the three ports of the junction. Equation (4) states that for three such excitations $[x]_1$, $[x]_2$, and $[x]_3$,* the reflected signals at each port are equal to the incident signals times a constant ϕ_1 , ϕ_2 , and ϕ_3 respectively. Since the ratio of reflected to incident signals at every port is ϕ_i , it is clear that

* Hence called eigen-excitations.

the eigenvalues are simply the reflection coefficients for the excitations. If the junction is lossless, the eigenvalues have a magnitude of unity $|\phi_i| = 1$, and are distinguishable from one another in phase only.

It has been shown by several authors that the eigen-excitations and eigenvalues are given by

$$[x]_1 = K\begin{bmatrix}1\\1\\1\end{bmatrix}; \qquad [x]_2 = K\begin{bmatrix}1\\1\ \exp(+j120^\circ)\\1\ \exp(-j120^\circ)\end{bmatrix};$$

$$[x]_3 = K\begin{bmatrix}1\\1\ \exp(-j120^\circ)\\1\ \exp(+j120^\circ)\end{bmatrix}; \qquad (5)$$

$$\begin{aligned}\phi_1 &= S_{11} + S_{12} + S_{13}\\ \phi_2 &= S_{11} + S_{12}\exp(+j120^\circ) + S_{13}\exp(-j120^\circ)\\ \phi_3 &= S_{11} + S_{12}\exp(-j120^\circ) + S_{13}\exp(+j120^\circ)\end{aligned} \qquad (6)$$

where K is a normalizing constant.[2,11-13] $[x]_1$ is the in-phase excitation with the signals in each port having equal magnitude and phase. $[x]_2$ and $[x]_3$ are the clockwise and anticlockwise rotating excitations respectively with the signals in each port having equal magnitudes but differing in phase by 120 degrees.

The simultaneous application of all three eigen-excitations to the junction is given by

$$K\begin{bmatrix}1\\1\\1\end{bmatrix} + K\begin{bmatrix}1\\1\ \exp(+j120^\circ)\\1\ \exp(-j120^\circ)\end{bmatrix} + K\begin{bmatrix}1\\1\ \exp(-j120^\circ)\\1\ \exp(+j120^\circ)\end{bmatrix} = 3K\begin{bmatrix}1\\0\\0\end{bmatrix}. \qquad (7)$$

This is equivalent to exciting one port only. If unity power is applied at this port, the normalizing constant K is 1/3. An input on one port is the most familiar form of excitation. As it is the sum of the three eigen-excitations, and as the S parameters are functionally related to the eigenvalues ϕ_i through equation (6), it is evident that the output in the three ports can be determined directly from the eigenvalues.

2.2 *Transmission and Return Losses*

The reflection and transmission coefficients, S_{pp} and S_{pq}, are given from equation (6) by

$$
\begin{aligned}
S_{11} &= 1/3\{\phi_1 + \phi_2 + \phi_3\} \\
S_{31} = S_{12} &= 1/3\{\phi_1 + \phi_2 \exp(-j120^\circ) + \phi_3 \exp(+j120^\circ)\} \\
S_{21} = S_{13} &= 1/3\{\phi_1 + \phi_2 \exp(+j120^\circ) + \phi_3 \exp(-j120^\circ)\}.
\end{aligned} \tag{8}
$$

If the junction eigenvalues are phase displaced from one another such that

$$
\begin{aligned}
\phi_1 &= 1 \\
\phi_2 &= 1 \exp j\theta_2 \\
\phi_3 &= 1 \exp j\theta_3 ,
\end{aligned} \tag{9}
$$

the return loss at port 1 and the transmission losses from ports 1 to 2 and 1 to 3 are given respectively by

$$
\begin{aligned}
&\text{Return Loss } (1 \rightarrow 1) = -20 \log |S_{11}| \\
&= -20 \log \{1/3 \,|\, 1 + \exp j\theta_2 + \exp j\theta_3 \,|\} \\
&= -20 \log \{1/3[3 + 2\operatorname{Cos}\theta_2 + 2\operatorname{Cos}\theta_3 + 2\operatorname{Cos}(\theta_2 - \theta_3)]^{\frac{1}{2}}\}
\end{aligned} \tag{10}
$$

$$
\begin{aligned}
&\text{Transmission Loss } (1 \rightarrow 2) = -20 \log |S_{21}| = -20 \log |S_{13}| \\
&= -20 \log \{1/3 \,|\, 1 + \exp j(\theta_2 + 120^\circ) + \exp j(\theta_3 - 120^\circ) \,|\} \\
&= -20 \log \{1/3[3 + 2\operatorname{Cos}(\theta_2 + 120^\circ) + 2\operatorname{Cos}(\theta_3 - 120^\circ) \\
&\quad + 2\operatorname{Cos}(\theta_2 - \theta_3 + 240^\circ)]^{\frac{1}{2}}\}
\end{aligned} \tag{11}
$$

$$
\begin{aligned}
&\text{Transmission Loss } (1 \rightarrow 3) = -20 \log |S_{31}| = -20 \log |S_{12}| \\
&= -20 \log \{1/3 \,|\, 1 + \exp j(\theta_2 - 120^\circ) + \exp j(\theta_3 + 120^\circ) \,|\} \\
&= -20 \log \{1/3[3 + 2\operatorname{Cos}(\theta_2 - 120^\circ) + 2\operatorname{Cos}(\theta_3 + 120^\circ) \\
&\quad + 2\operatorname{Cos}(\theta_2 - \theta_3 - 240^\circ)]^{\frac{1}{2}}\}.
\end{aligned} \tag{12}
$$

These losses are shown plotted for θ_2 and θ_3 in the range zero to 360 degrees in Figs. 1, 2, and 3. As was shown by Auld, circulation occurs when the eigenvalues are mutually displaced by 120 degrees.[2] This condition is satisfied both at X and Y in Figs. 1, 2, and 3, and these points represent the opposite senses of circulation. At X, anticlockwise circulation takes place with

$$
\begin{aligned}
\phi_1 &= 1 \\
\phi_2 &= 1 \exp(+j120^\circ) \\
\phi_3 &= 1 \exp(-j120^\circ),
\end{aligned} \tag{13}
$$

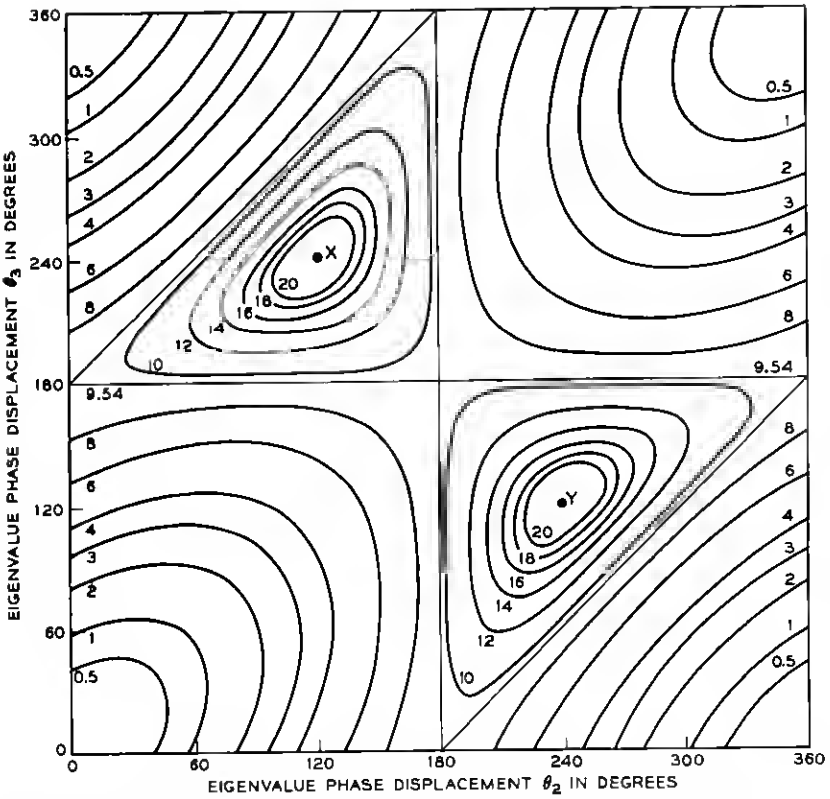

Fig. 1—The return loss in decibels on port 1 is shown as a function of the phase angles between the eigenvalues. The curves are the locii of constant loss.

and at Y, clockwise circulation occurs with

$$\begin{aligned} \phi_1 &= 1 \\ \phi_2 &= 1 \exp(-j120^\circ) \\ \phi_3 &= 1 \exp(+j120^\circ). \end{aligned} \tag{14}$$

Figure 4 schematically displays how circulation is achieved in terms of the eigen-excitations and eigenvalues. The inner and outer circles on each port represent the ingoing and outgoing eigen-excitation components respectively. The ingoing components cancel in ports 2 and 3 and sum in port 1. Only port 1 is then excited. The eigenvalues are the ratios of the outgoing to ingoing wave components for each

eigen-excitation. If the eigenvalue arguments are $\angle\phi_1 = 0°$, $\angle\phi_2 = -120°$, and $\angle\phi_3 = +120°$ as in Figure 4a, the outgoing components cancel in ports 1 and 3 and sum in port 2. The junction then circulates in the clockwise direction. If the eigenvalue arguments are $\angle\phi_1 = 0°$, $\angle\phi_2 = +120°$, and $\angle\phi_3 = -120°$ as in Figure 4b, the outgoing components cancel in ports 1 and 2 and sum in port 3. The junction now circulates in the anticlockwise direction.

Referring again to Figs. 1, 2, and 3, it is interesting to note that the return loss on the input port and the transmission loss to the isolated port are identical only when two of the three eigenvalues are mutually displaced by 120 degrees. Figure 5 shows the losses when θ_2 is fixed at 240 degrees and θ_3 is allowed to vary from 80 degrees to 160 degrees.

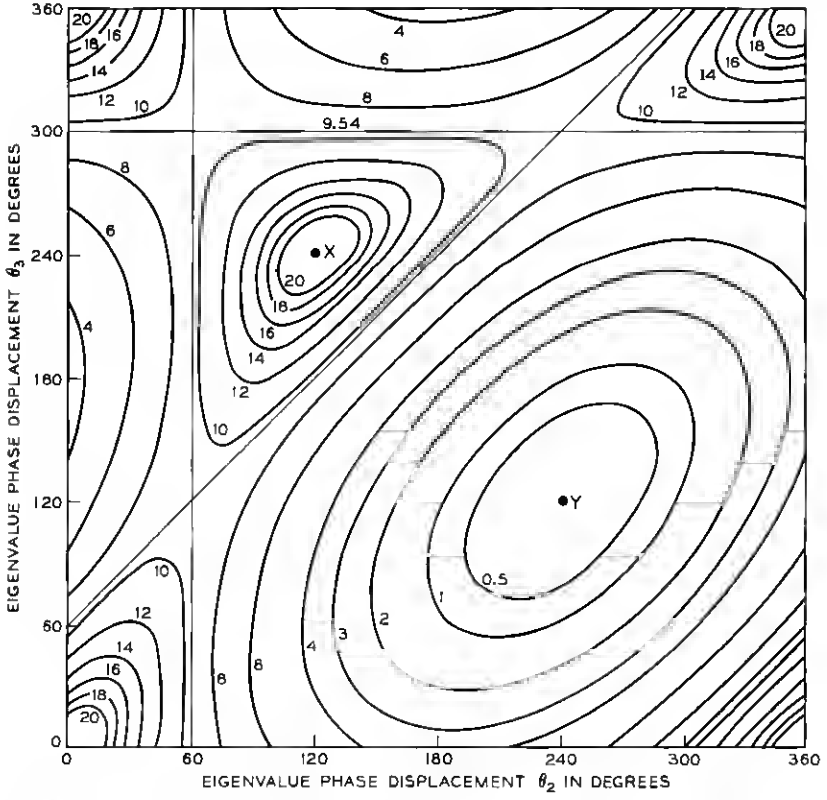

Fig. 2—The transmission loss in decibels from port 1 to port 2 is shown as a function of the phase angles between the eigenvalues. The curves are the locii of constant loss.

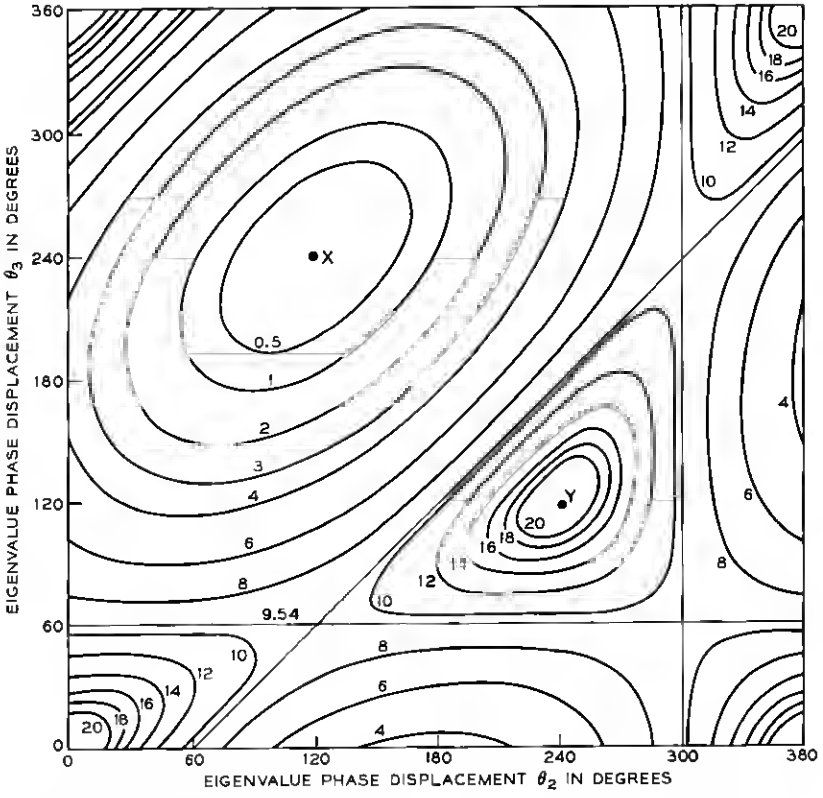

Fig. 3—The transmission loss in decibels from ports 1 to 3 is shown as a function of the phase angles between the eigenvalues. The curves are the locii of constant loss.

The isolation and return loss are both reduced to 30 dB and 20 dB when θ_3 deviates by ± 5.5 degrees and ± 17 degrees respectively from its 120 degrees relative position. This indicates the approximate limits on the phase of the eigenvalues for a satisfactory circulator characteristic.

For broadband circulation, the symmetrically disposed junction components must be arranged so that the eigenvalues are correctly displaced over a wide frequency range. The phase-frequency responses of the three eigenvalues and their sensitivities to various parameters are then important characteristics in broadband circulator design. A circuit capable of examining the eigenvalues individually is described in the following section.

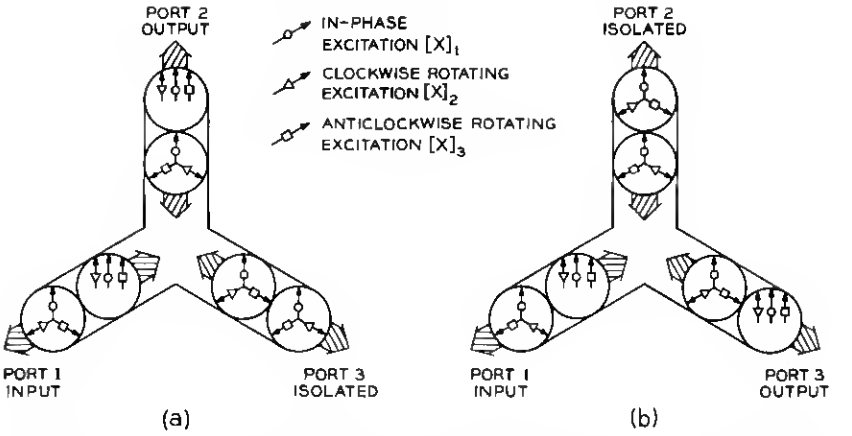

Fig. 4—A phase displacement of 120 degrees between the eigenvalues results in circulation. In (a), ϕ_2 is phase retarded and ϕ_3 phase advanced for clockwise circulation. In (b), ϕ_2 is phase advanced and ϕ_3 phase retarded for anticlockwise circulation.

III. EIGENVALUE MEASUREMENTS

For maximum utilization a circuit is required that is capable of displaying the magnitudes and phases of the three eigenvalues over a full waveguide band. Several eigenvalue measurement techniques are available in the literature, but only a few seem capable of operating on a swept frequency basis.[11] One method is to measure the reflection and transmission coefficients S_{11} , S_{12} , and S_{13} , and to determine the eigenvalues directly from equation (6). The computation involved,

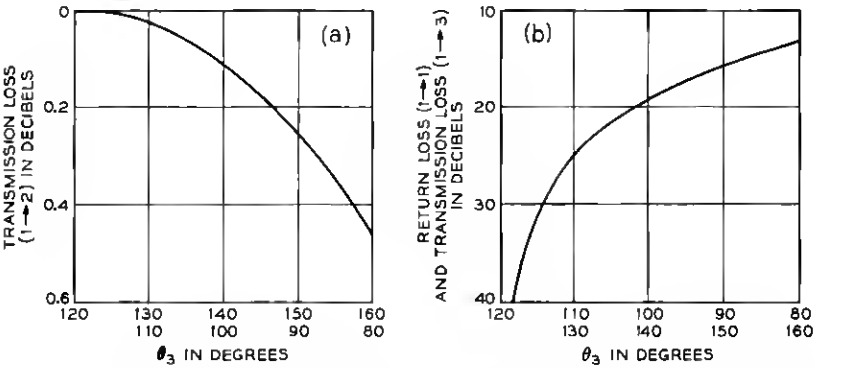

Fig. 5—(a) Transmission loss from ports 1 to 2 and (b) transmission loss from ports 1 to 3 and return loss on port 1 as a function of θ_3 with θ_2 fixed at 240 degrees.

however, is rather extensive, and it does not provide a real time display. The technique to be reported here is similar to a method proposed by F. M. Magalhaes for synthesizing lumped element circulators.[14] The three eigen-excitations are individually applied to the junction, and the eigenvalues are determined from the reflection coefficients on any one port.

A circuit capable of such measurements at X-band is shown in Fig. 6. The 3-way power divider couples signals of equal magnitude to the three arms connected to the Y-junction. These arms are of the same mechanical length, and are made up of identical components which track in phase and loss as a function of frequency. The 20-dB attenuators prevent errors due to circulating energy in the waveguide circuit, and the variable attenuators equalize any loss differences in the three arms. The phase shifters are adjustable for the in-phase, and rotating eigen-excitation conditions.

To avoid the use of two couplers on each arm for reflection coefficient measurements, the eigenvalues are determined by sampling the incident signal on one port and the reflected signal on the other. The coupler on arm 3 is terminated, and is included only for phase equalization. The other two couple the incident and reflected signals on arms 1 and 2 respectively to a network analyzer and XY recorder. The components then measured for the three eigen-excitations are ϕ_1 , $\phi_2 \exp(+j120°)$, and $\phi_3 \exp(-j120°)$ respectively. A zero-phase adjustment of 0°, $-120°$, and $+120°$ on the analyzer enables ϕ_1 , ϕ_2 , and ϕ_3 , respectively, to be displayed on the XY recorder. An alternative method which avoids this zero-phase adjustment is discussed in the Appendix.

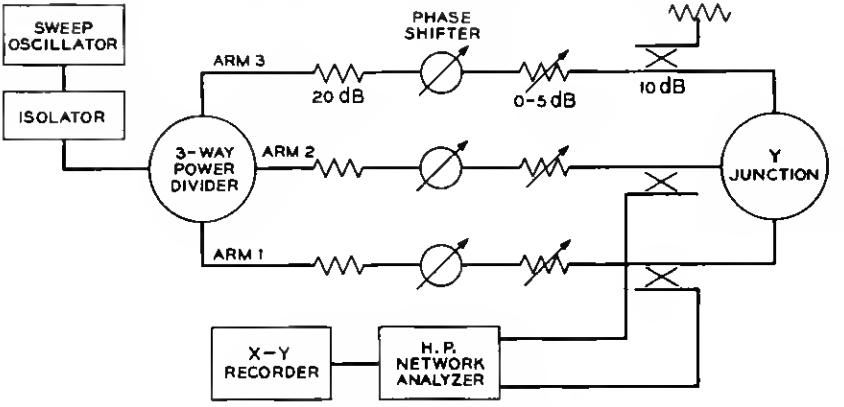

Fig. 6—The eigenvalue measuring set.

IV. RESULTS

The Y-junction used in the experimentation was made from 0.900-inch wide and 0.450-inch high X-band waveguide. Most commonly used waveguides have this 2 to 1 aspect ratio. Its selection here was motivated by the desire to scale synthesized circulators to other frequency bands. For compatibility with the measuring set, broadband transitions to standard 0.400-inch high guide were used on each port. The junction was milled in brass, and threaded plugs at the center of the lid facilitated the interchange of ferrite posts. Some plugs had a finely threaded hole at the center so that metallic pins of various diameters could be introduced along the junction symmetry axis. The reflection coefficient measurements were referenced to planes on the three ports 0.437 inch from the junction center. The polarity of the biasing field was kept constant, and its magnitude was determined using a Hall effect probe with the ferrite post removed.

Eigenvalue measurements were made on the junction with a number of different ferrite geometries enclosed. Several different ferrites were also used. Their saturation magnetizations and loss tangents were small enough to avoid magnetic low field losses and to minimize dielectric losses. The junction was then essentially free of dissipation, and the eigenvalue magnitudes were very close to unity. Only the phases of the eigenvalues need then be considered. Most of the results were taken on Trans-Tech magnesium based TT1-1500 ferrite. This was available in large quantities at the time, and was selected for this reason only. It had the following properties:

Saturation magnetization, $4\pi M_s = 1500$ Gauss
Dielectric constant, $\epsilon = 12$
Dielectric loss tangent, Tan $\delta = 0.00025$
Line width, $\Delta H = 180$ Oersted.

Normally a ferrite with up to twice this saturation magnetization would be selected for use in broadband X-band circulators. Care was taken to demagnetize each ferrite sample before it was used in the junction.

4.1 *Junction with a Full Height Ferrite*

Consider the junction with a full height ferrite post, and excited from the connecting waveguides by the dominant TE_{10} mode. The electric field is everywhere parallel to the symmetry axis, and no variations occur in this direction. The junction modes are then of the $TM^{*}_{\pm m,n,0}$ type. Integer m indicates the number of full period

* Transverse to the symmetry axis.

azimuthal variations with the field pattern rotating in the clockwise (+) and anticlockwise (−) directions. Integer n indicates the number of half-period radial variations. The $TM_{\pm m,n,0}$ ($m > 0$) rotating modes are excited by the $[x]_2$ and $[x]_3$ eigen-excitations. Their magnetic field components are circularly polarized in opposite directions at the junction center. The $TM_{0,n,0}$ in-phase modes are excited by the $[x]_1$ eigen-excitation. Their magnetic field components are zero at the junction center.

The eigenvalue phase-frequency response of such a junction with a 0.260-inch diameter ferrite is shown in Fig. 7. Only the rotating $TM_{\pm 1,1,0}$ modes are resonant within band. The $[x]_2$ eigen-excitation couples to the $TM_{+1,1,0}$ mode, and the $[x]_3$ eigen-excitation couples to the $TM_{-1,1,0}$ mode. With no field applied, $\angle\phi_2$ and $\angle\phi_3$ are identical, and both resonances occur at 9.5 GHz. As field is applied, the degeneracy is removed and the resonances split apart. This occurs because the magnetized ferrite presents different permeabilities to the two circularly

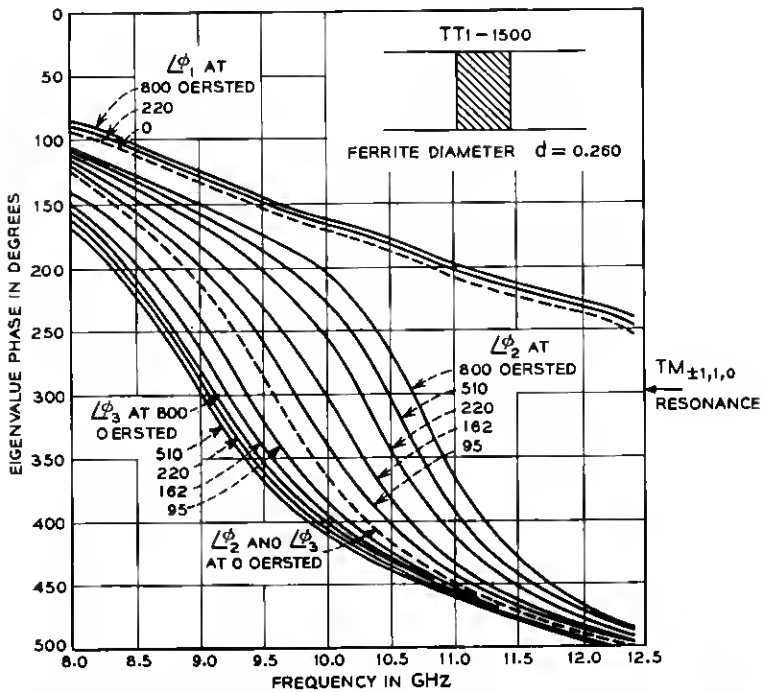

Fig. 7—The eigenvalue phase-frequency response of a junction with a full height ferrite post and various biasing fields.

polarized modes. The resonant frequency of the $TM_{+1,1,0}$ mode increases with field while the resonant frequency of the $TM_{-1,1,0}$ mode decreases until the ferrite is saturated, and then increases as shown in Fig. 8. An identical phenomenon was observed for the stripline circulator by Fay and Comstock in 1965.[4] The phases of eigenvalues ϕ_2 and ϕ_3 are significantly displaced only in the immediate vicinity of the resonances where the fields in the ferrite are at a maximum. None of the in-phase modes are resonant within band, and $\angle\phi_1$ is only slightly modified by the applied field. The transmission losses from ports 1 to 2 and ports 1 to 3 are determined from the measured eigenvalues using equations (11) and (12). They are shown in Fig. 9. The eigenvalues are correctly displaced for circulation at 10.3 GHz when the applied field is 220 Oersted. The 20-dB isolation bandwidth is 350 MHz (3.4 percent).

The circulating frequency may be adjusted by varying the $TM_{\pm1,1,0}$ resonances. This may be accomplished over a limited range by using ferrite with different dielectric constants, as shown in Fig. 10. The resonant frequency of the zero field $TM_{\pm1,1,0}$ mode varies inversely as the square root of the dielectric constant, and decreases from 11.2 GHz to 10 GHz as the dielectric constant is increased from 11.3 to 14.5. Over a wider band, changing the ferrite post diameter is much more effective. The zero field resonance varies inversely with the post diameter, and sweeps from 12.4 GHz to 8.0 GHz in Fig. 11 as the diameter is increased from 0.200 inch to 0.300 inch. The slope of $\angle\phi_1$ is essentially unchanged over the range in both cases, and the circulator bandwidth remains nearly constant.

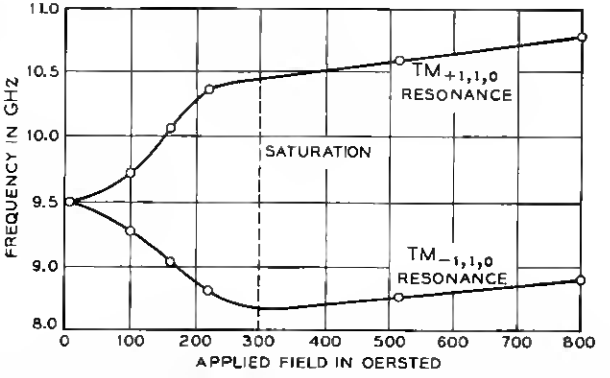

Fig. 8—The splitting of the $TM_{+1,1,0}$ and $TM_{-1,1,0}$ resonances in a junction with a full height ferrite post as a function of the biasing field. The results are obtained from Fig. 7.

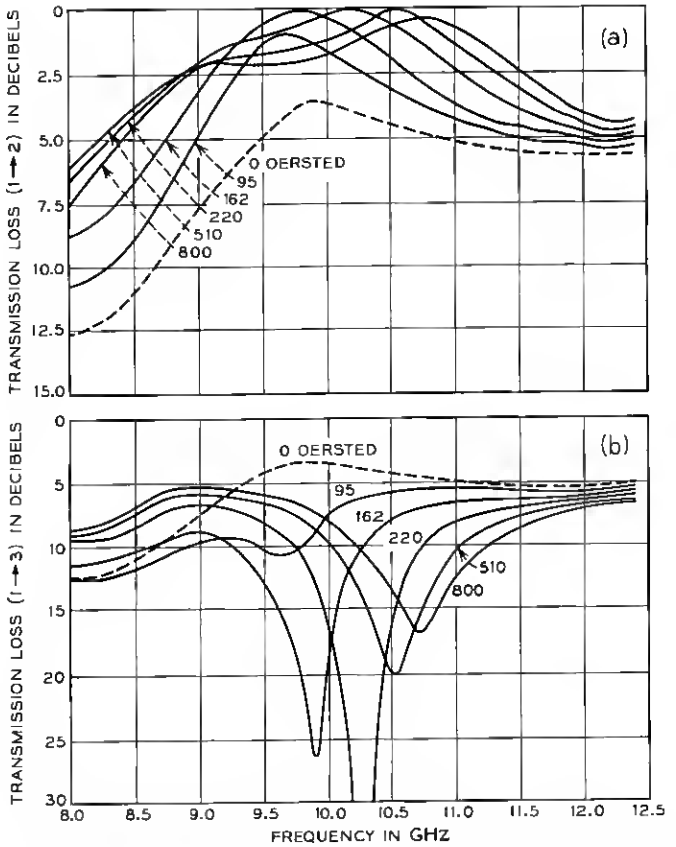

Fig. 9—Transmission losses from (a) ports 1 to 2 and (b) ports 1 to 3 in a junction with a full height post for various biasing fields. The results are obtained from Fig. 7 and equations (11) and (12).

Circulation is also possible in the vicinity of the higher order $TM_{\pm 2,1,0}$ mode which comes within band when the ferrite diameter is larger than 0.320 inch. It is closely accompanied by the in-phase $TM_{0,2,0}$ mode. The $[x]_2$ eigen-excitation now couples to the $TM_{-2,1,0}$ mode, and the $[x]_3$ eigen-excitation to the $TM_{+2,1,0}$ mode. For the same polarity of biasing field, the splitting occurs in opposite directions from the splitting in the vicinity of the $TM_{\pm 1,1,0}$ modes. The $TM_{+2,1,0}$ resonant frequency decreases with field while the $TM_{-2,1,0}$ resonant frequency increases as shown in Fig. 12. The effect was also predicted by Fay and Comstock in 1965.[4]

4.2 *Junction with a Centrally Pinned, Full Height Ferrite*

It was shown by K. Kurokawa that the electric field components of the in-phase excitation sum at the junction center while those of the rotating excitations mutually cancel.[13] This feature can be used to provide an independent control for the phase of eigenvalue ϕ_1 .

A thin metallic pin inserted along the symmetry axis does not affect the rotating modes, and leaves $\angle\phi_2$ and $\angle\phi_3$ unchanged. It significantly affects the phase of ϕ_1 by introducing $TM_{0,n,z}$ type modes. These have components of electric field perpendicular to the symmetry axis, and resonate between the discontinuity at the open end of the pin and the broadwall of the waveguide junction. They are demonstrated in Fig. 13. As the pin is inserted into the junction, two resonances sweep across the band from the high end. They occur when the pin is approximately one quarter and three quarter wavelengths long in the ferrite medium. They are the $TM_{0,1,\delta}$ and $TM_{0,1,1+\delta}$ ($\delta \approx 0.5$) resonances respectively. When the pin extends fully across the junction, continuity in the direction parallel to the symmetry axis is restored and the resonances disappear. The phases of ϕ_2 and ϕ_3 are essentially unaffected by the pin position.

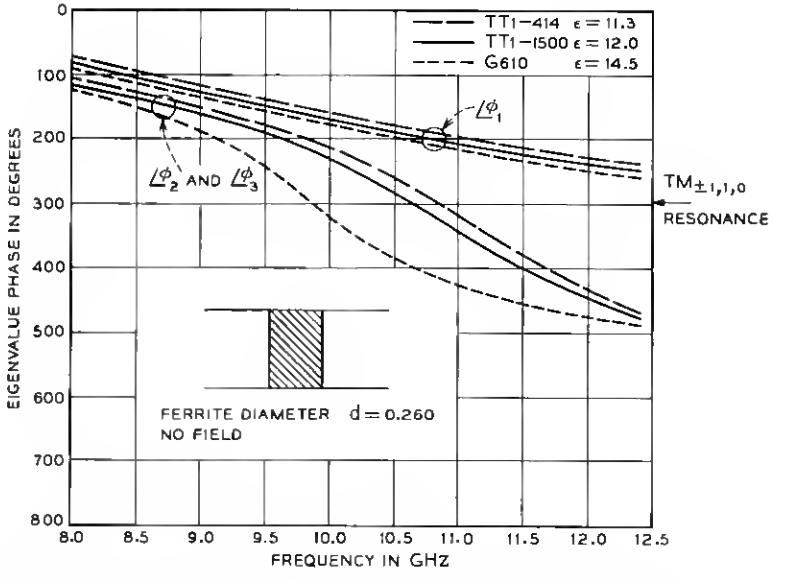

Fig. 10—The eigenvalue phase-frequency response of a junction with a full height ferrite post with various dielectric constants. No biasing field is applied.

The $TM_{0,n,z}$ resonances are not only a function of the ferrite diameter, ferrite dielectric constant, and pin height but also of the ferrite hole and pin diameters. They move to higher frequencies as these diameters are made larger as shown in Fig. 14. This is expected since both the

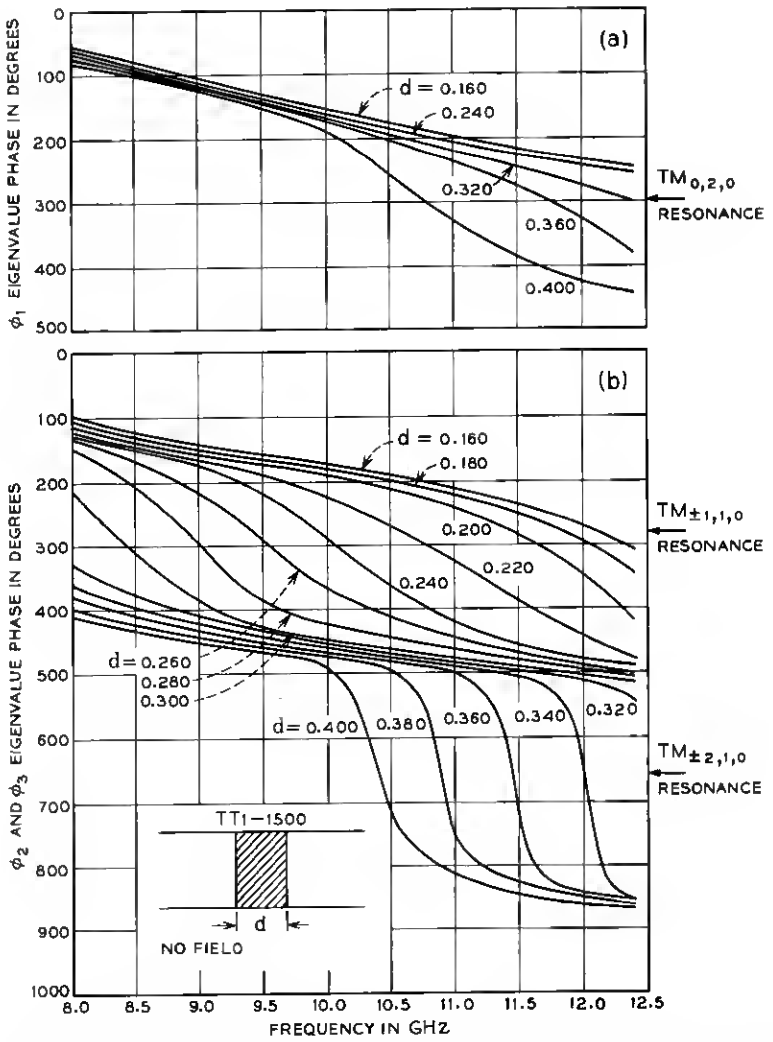

Fig. 11—The eigenvalue phase-frequency response of a junction with a full height ferrite post of various diameters. The results display (a) the lower-order $TM_{0,n,0}$ modes in $\angle\phi_1$, (b) the lower-order $TM_{\pm m,n,0}$ modes in $\angle\phi_2$ and $\angle\phi_3$.

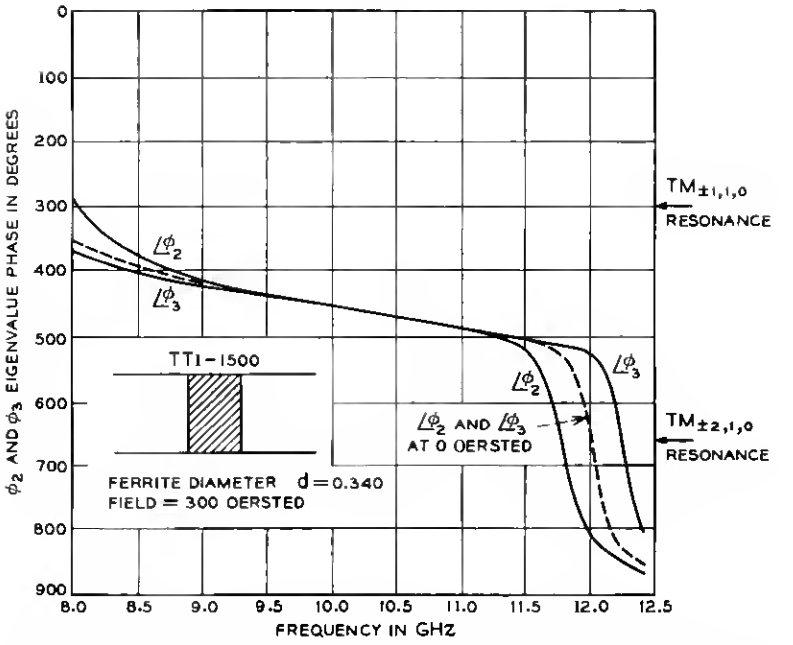

Fig. 12—The eigenvalue phase-frequency response of a junction with a full height ferrite post showing the $TM_{\pm 1,1,0}$ and $TM_{\pm 2,1,0}$ resonant modes splitting in opposite directions with field.

larger hole and pin tend to exclude fields from the ferrite, and thereby increase the frequency at which the pin resonates. The change in the phases of ϕ_2 and ϕ_3 is initially very small. However, when the pin diameter reaches 0.098 inch, a resonance occurs at 10.8 GHz. The discontinuity at the open end of the pin is now sufficiently large to excite rotating modes that resonate along the ferrite axis. These modes are of the $HE_{\pm m,n,z}$ type. They are also excited by a partial height ferrite, and are discussed in detail in Section 4.4.

The hole in the ferrite has other effects that have to be considered. The permeability difference for the rotating modes is a maximum at the junction center where the magnetic fields are circularly polarized. At the ferrite edge where the polarization is elliptical, the permeability difference is much less. Removing ferrite from the center then reduces the phase displacement of ϕ_2 and ϕ_3 with field as shown in Fig. 15. The demagnetized curves also indicate that the resonances move to higher frequencies as the hole diameter is made larger. This is due to the reduction in the effective dielectric constant of the ferrite cylinder.

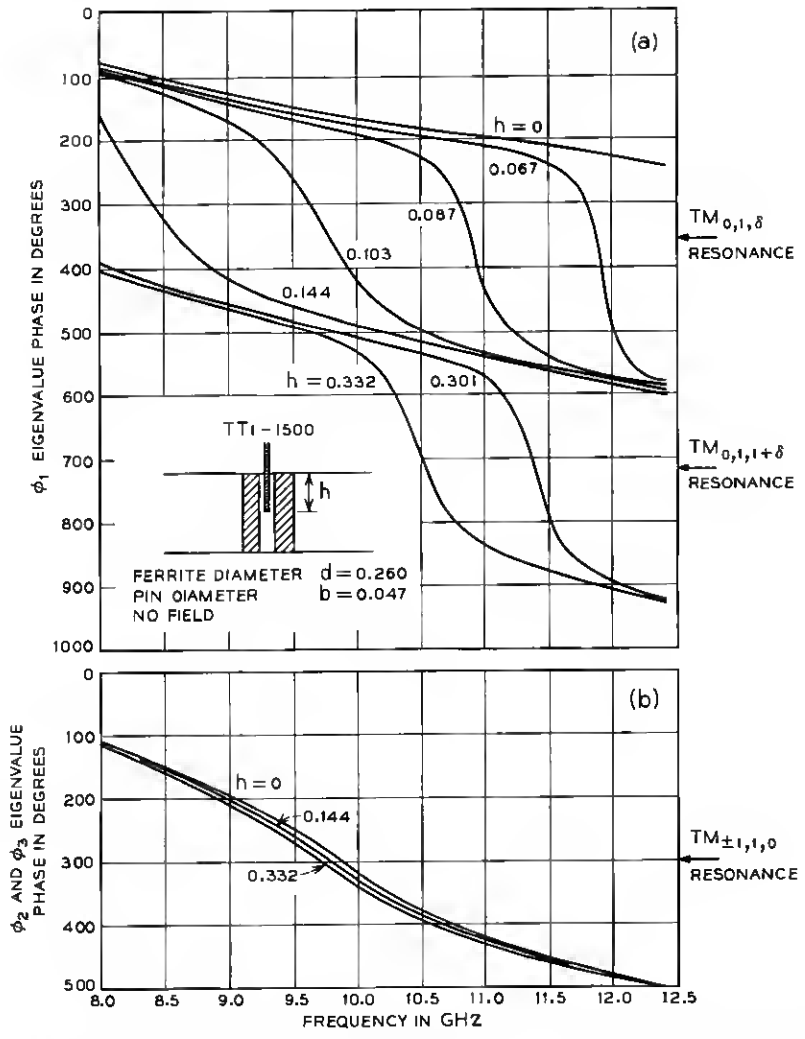

Fig. 13—The eigenvalue phase-frequency response of a junction with a centrally pinned ferrite post. The results display (a) the $TM_{0,1,\delta}$ and $TM_{0,1,1+\delta}$ resonances that are induced in $\angle\phi_1$ by the variable height pin and (b) how $\angle\phi_2$ and $\angle\phi_3$ remain unchanged.

The independent control on $\angle\phi_1$ provided by the thin pin is very useful for circulator synthesis as is demonstrated in Fig. 16. The ferrite is magnetized to separate $\angle\phi_2$ and $\angle\phi_3$ hy 120 degrees at 9.4 GHz. A pin-induced $TM_{0,1,\delta}$ resonance is then adjusted to position $\angle\phi_1$ 120 degrees away from both $\angle\phi_2$ and $\angle\phi_3$ at the same frequency. The resultant circulator has a 20-dB isolation handwidth of 600 MHz

(6.4 percent). The bandwidth improvement from the non-pinned junction is due to the $TM_{0,1,\delta}$ resonance. The slope of $\angle\phi_1$ in its vicinity more nearly matches the slopes of $\angle\phi_2$ and $\angle\phi_3$. If all three resonances had lower and more comparable eigenvalue phase-frequency slopes,

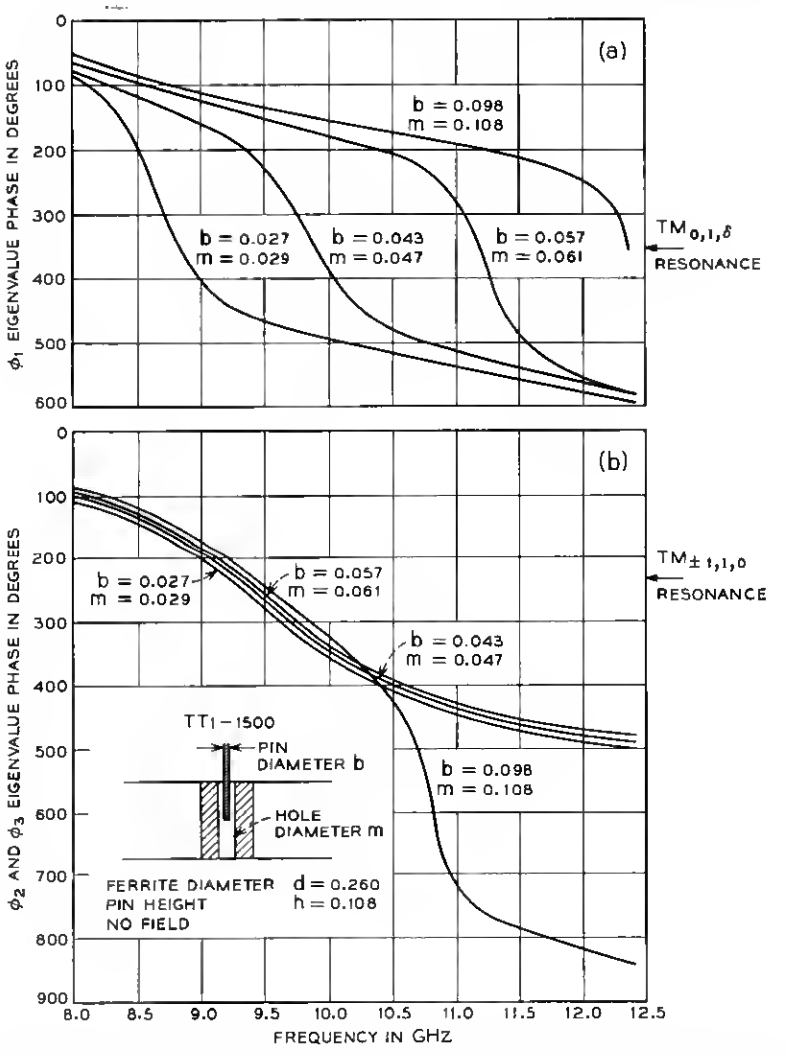

Fig. 14—The eigenvalue phase-frequency response of a junction with a full height ferrite post and containing various diameter holes and various diameter axial pins. In (a), the $TM_{0,1,\delta}$ resonance in $\angle\phi_1$ increases in frequency as the pin diameter is made larger. In (b), $\angle\phi_2$ and $\angle\phi_3$ are unaffected until the pin is sufficiently large to excite axially resonating $HE_{\pm m,n,z}$ modes.

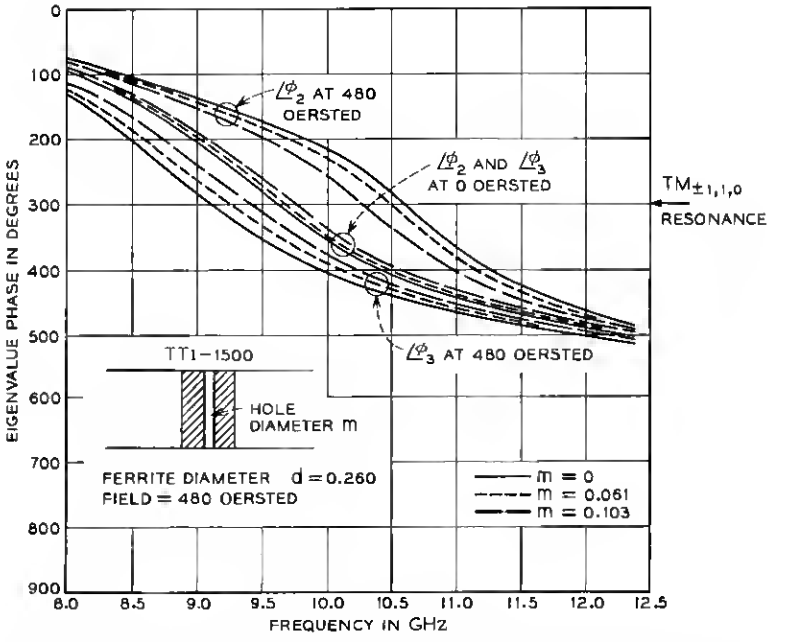

Fig. 15—The eigenvalue phase-frequency response of a junction with a full height ferrite post and with different diameter holes along its axis. The results are displayed both with and without field.

the bandwidth improvement would have been even more substantial.

4.3 *Junction with a Partial Height Ferrite*

It was recently proposed that some circulators with a partial height ferrite operate in a turnstile fashion with rotating modes propagating along the ferrite axis.[15] These modes are excited by the dielectric discontinuity at the open end of the ferrite, and are characterized by electric field components perpendicular to the symmetry axis. When the rotating eigen-excitations are applied, the signals from the three ports induce three such transverse components on the ferrite, each space displaced from the other by 120 degrees. Together they couple to the $HE_{\pm m,n,z}$ series of modes that resonate along the ferrite axis. For the in-phase excitation the three transverse components are in phase with one another, but the 120 degrees spatial separation results in cancellation at the junction center. They couple to the $TM_{0,n,z}$ series of modes as before.

Figure 17 demonstrates these effects on a 0.300-inch diameter ferrite.

The full height results are shown dotted. The $TM_{\pm 1,1,0}$ diametric resonance is centered at 8.2 GHz, and no $TM_{0,n,0}$ mode is resonant within band. A small reduction in the ferrite height produces rapid 360-degree phase transitions in $\angle\phi_2$ and $\angle\phi_3$ at 8.9 GHz and 11.2 GHz. These are the $HE_{\pm 1,1,1+\delta}$ and $HE_{\pm 1,1,2+\delta}$ axial resonances, respectively. They resonate between the open end of the ferrite on the one side, and the broadwall of the waveguide junction on the other. As the ferrite height is reduced, the resonances move to higher frequencies. Below 0.250 inch, the lowest-order $HE_{\pm 1,1,\delta}$ resonance comes within band. The ferrite is approximately an odd number of quarter wavelengths long ($\delta \approx 0.5$) at these HE resonate frequencies. The physical dimensions are in good agreement with those predicted for the resonances when the ferrite is assumed to be a dielectric rod waveguide with dielectric constant $\epsilon = 12$ and relative permeability $\mu \approx 1$.

Recalling from Section 4.2 that a resonance is necessary to separate the phases of ϕ_2 and ϕ_3, circulation now becomes possible in the vicinity of both the $HE_{\pm m,n,\delta}$ and $TM_{\pm m,n,0}$ resonances. The bandwidths are comparable in both cases. Further, as the resonances are differentially affected by the ferrite height, they are easily "staggered" for a larger

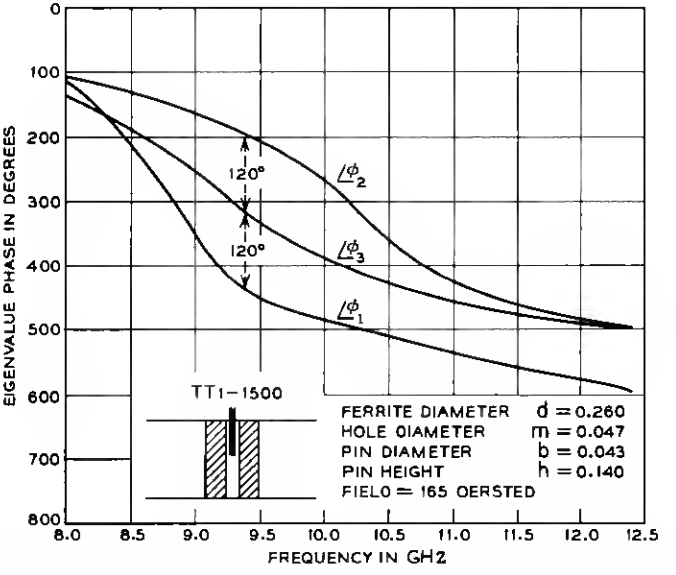

Fig. 16—The eigenvalue phase-frequency response of a junction with an axially pinned ferrite post. The biasing field and pin have been adjusted for circulation at 9.4 GHz.

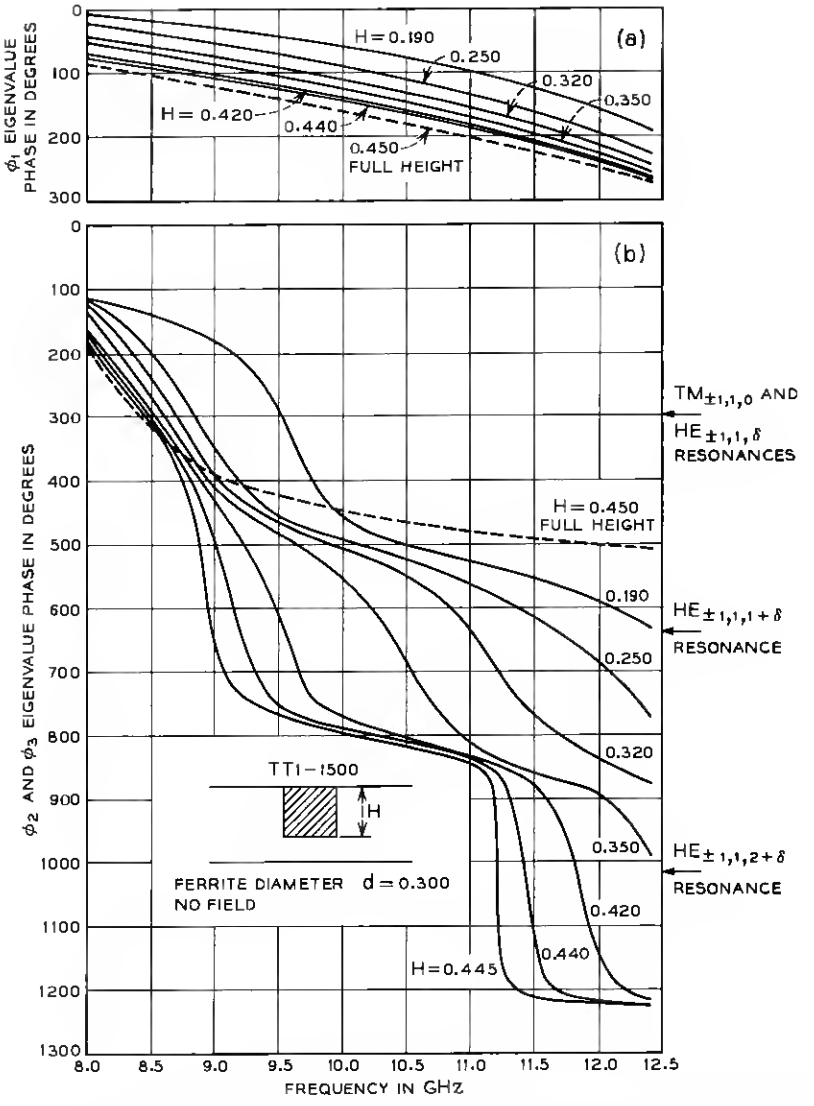

Fig. 17—The eigenvalue phase-frequency response of a junction with a partial height ferrite post. The ferrite diameter is selected to position the $TM_{\pm1,1,0}$ resonance at the low end of the band. The results show (a) the phase of ϕ_1 is only slightly changed as the ferrite height is reduced, (b) the axially resonating $HE_{\pm m,n,z}$ modes in $\angle\phi_2$ and $\angle\phi_3$ increase in frequency.

bandwidth. Clearly the eigenvalue displacement with field must be in the same direction in both cases. This is automatically satisfied if the modes have the same azimuthal, m, variation. The results for one such "stagger-tuned" circulator are shown in Fig. 18. The $TM_{\pm 1,1,0}$ resonance is centered at 8.4 GHz, and the $HE_{\pm 1,1,1+\delta}$ resonance at 9.9 GHz. With biasing field applied, $\angle\phi_2$ and $\angle\phi_3$ are now displaced by 120 degrees over a wider band. A $TM_{0,1,\delta}$ pin-induced resonance provides the correct displacement and slope for $\angle\phi_1$. The resultant circulator has a 20-dB isolation bandwidth of 700 MHz (7.6 percent).

The coupling to the HE modes may be from one side of the ferrite

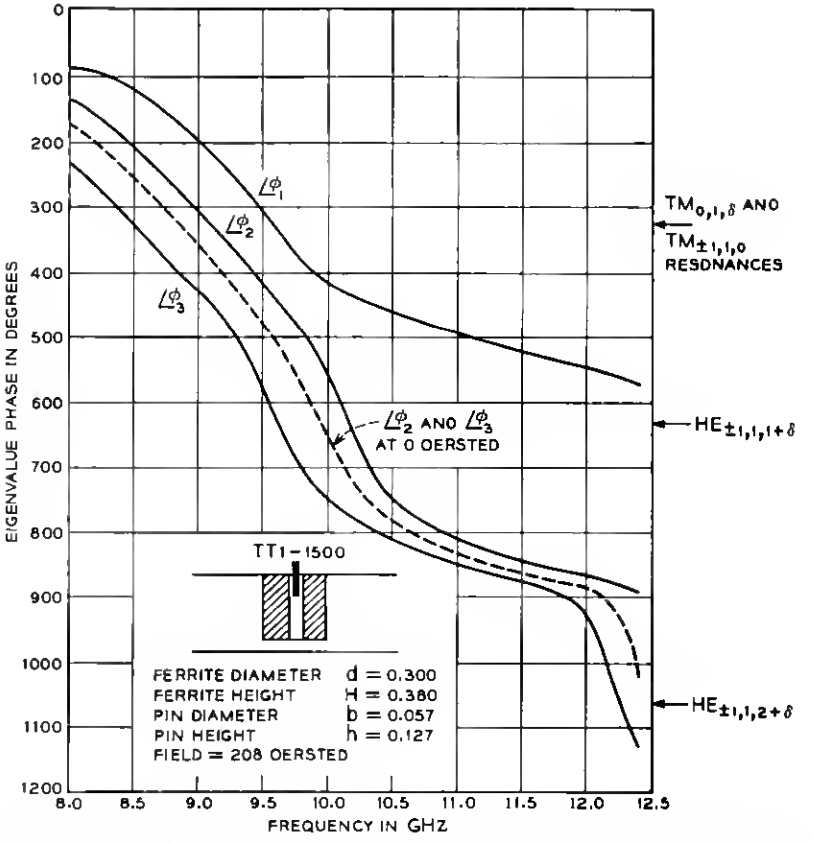

Fig. 18—The eigenvalue phase-frequency response of a junction with a partial height and pinned ferrite. The ferrite height and diameter have been selected to "stagger" the $TM_{\pm 1,1,0}$ and $HE_{\pm 1,1,1+\delta}$ modes, and the $TM_{0,1,\delta}$ pin-induced resonance has been adjusted for circulation at 9.3 GHz.

only or from both sides simultaneously. This provides for an additional variation. In the double-sided case, low dielectric constant spacers support the ferrite on either side, and provide the discontinuity necessary to launch the axially propagating modes. The resonances now occur when the ferrite is approximately an integral number of half wavelengths long ($\delta \approx 1$), as shown in Fig. 19. The Q-factor is also reduced because of the larger coupling.

4.4 *Junction with a Transformed Ferrite*

The bandwidths of the circulators synthesized so far are less than 10 percent. The limitation is imposed by the junction resonances. The band over which the required displacement is achieved is confined

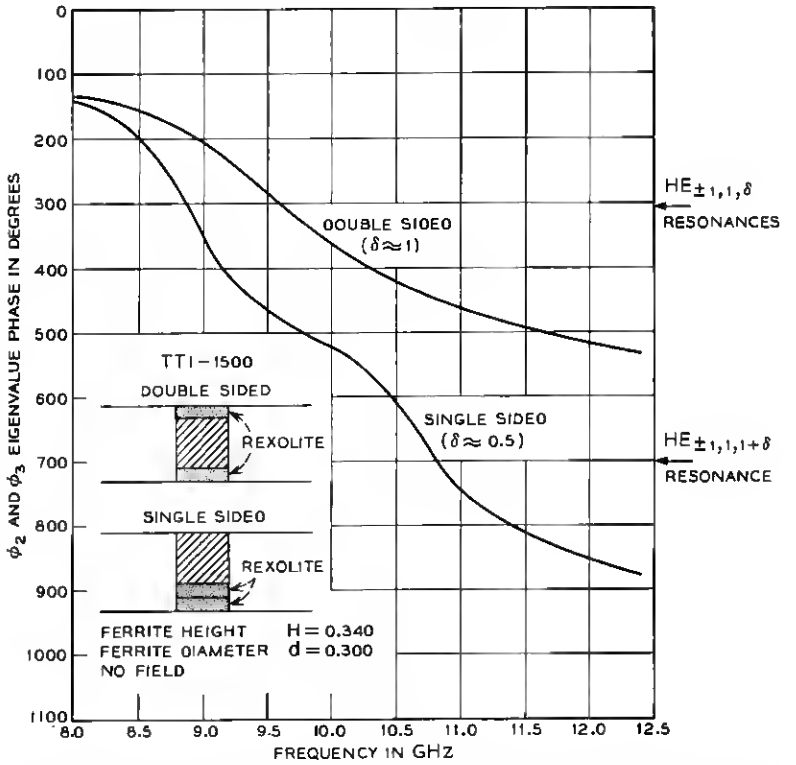

Fig. 19—The phase-frequency response of ϕ_2 and ϕ_3 for a junction with a partial height ferrite of both the single- and double-sided type. In the single-sided case, the HE resonances occur when the ferrite is approximately an integral number of quarter wavelengths long ($\delta \approx 0.5$). In the double-sided case, they occur when the ferrite is approximately an integral number of half wavelengths long ($\delta \approx 1$).

to the immediate vicinity of the rotating mode resonances. Staggering $HE_{\pm m,n,z}$ and $TM_{\pm m,n,0}$ resonances as in Fig. 18 provides little relief. The resonance of the in-phase eigen-excitation then limits the bandwidth.

Several methods exist for overcoming this restriction. The most commonly used technique is to introduce a quarter-wave transformer into the junction. This may be formed from a dielectric cylinder surrounding the ferrite, or from a metallic pedestal placed between the ferrite and the broadwall of the waveguide junction. Only the metal transformer type is considered here. Its effect on the eigenvalues is shown in Fig. 20. The radial difference, w, between the ferrite and the transformer is one quarter wavelength in free space at 9.2 GHz. The transformer step height is t. With no transformer present ($t = 0$), the $TM_{\pm 1,1,0}$ resonance is centered at 9.5 GHz. As t is increased, the phase-frequency responses of ϕ_2 and ϕ_3 become more linear. An optimum is reached when t is approximately 0.130 inch. The linearity permits a more constant displacement of $\angle\phi_2$ and $\angle\phi_3$ with field as shown in Fig. 21. Referring again to Fig. 20, a spurious resonance moves into the band when $t > 0.130$ inch. This is an evanescent mode associated with the transformer. Little energy is coupled to the ferrite in its vicinity, and no displacement occurs when field is applied. Figure 20 also displays the effect of the transformer on the phase of ϕ_1 . For $t = 0$, $\angle\phi_1$ is essentially linear with frequency. As t is increased, $\angle\phi_1$ takes on a curvature suggesting a low-Q resonance near or just below the lower end of the band.

The transformer and full height ferrite geometry of Fig. 20 does not directly lend itself to broadband circulation. The transformer cannot easily equalize the phase-frequency slopes of the eigenvalues, and simultaneously arrange for their correct displacement. Another degree of freedom is required for the adjustment of the eigenvalues, and this accounts for the use of partial height ferrites in many existing designs. From Section 4.3, it is apparent that a central conducting pin would also provide the additional degree of freedom required.

An example in the use of the pin is shown in Fig. 22. Except for the hole in the ferrite center and the pin, the junction is identical to the one shown in Fig. 21. The transformer linearizes $\angle\phi_2$ and $\angle\phi_3$ in the vicinity of the $TM_{\pm 1,1,0}$ resonance at 9.5 GHz, and a biasing field is applied to displace these eigenvalues by 120 degrees over a wide band. The pin-induced $TM_{0,1,\delta}$ resonance in $\angle\phi_1$ is likewise linearized by the transformer, and its position adjusted for optimum circulation. The 20-dB isolation bandwidth is 1.35 GHz (15.2 percent).

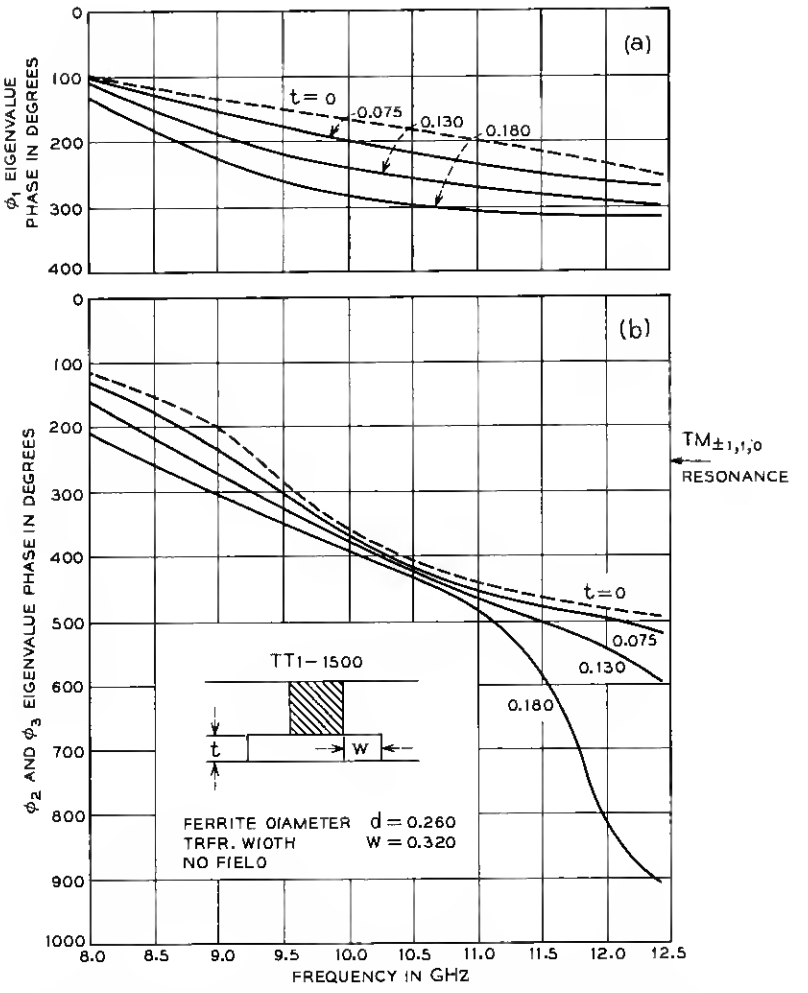

Fig. 20—The eigenvalue-phase frequency response of a junction with a full height ferrite post and different height transformers. The results show (a) the curvature in $\angle\phi_1$ as the transformer height is increased and (b) the linearization of $\angle\phi_2$ and $\angle\phi_3$ in the vicinity of the $TM_{\pm 1,1,0}$ resonance.

The effect of the transformer is essentially the same for both the $TM_{\pm m,n,0}$ and $HE_{\pm m,n,z}$ modes. Recalling that these modes are differentially affected by the ferrite height, a very wideband circulator of this nature then becomes possible by having both a $TM_{\pm m,n,0}$ and a $HE_{\pm m,n,z}$ resonance within band. With a suitable transformer the

eigenvalue linearization can extend into both resonance regions. The proper combination of pin height, transformer, and applied field can also provide linearization for a pin-induced resonance in $\angle\phi_1$, and the correct mutual eigenvalue displacement over this extended range. Such a circulator synthesized in standard 0.900-inch wide and 0.400-inch high X-band waveguide is shown in Fig. 23. A slight recess in the transformer directly beneath the ferrite provides the desired coupling for the $HE_{\pm 1,1,1+\delta}$ mode, and a sleeve around the transformer provides minor adjustments for an optimum 20-dB bandwidth. The losses calculated from the eigenvalue phases using equations (11) and (12) are compared with those measured on a transmission loss test set in Fig. 24. The 20-dB isolation bandwidth is 3.1 GHz (31 percent) centered at 10 GHz. It nearly extends over the full waveguide band.

V. CONCLUSIONS

Examining a symmetrical nonreciprocal 3-port junction in terms of its eigenvalues is an extremely useful method for determining the mode of operation of a Y-circulator. It provides a direct relation between the scattering matrix theory, the inner junction modes, and the resultant device characteristics. For many circulator geometries, the exact nature

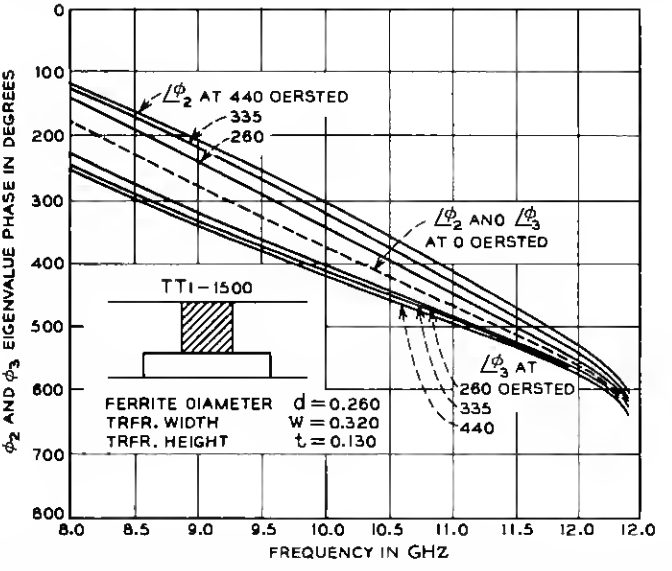

Fig. 21—The phase-frequency response of ϕ_2 and ϕ_3 for a junction with a transformer and full height ferrite post. The linearization due to the transformer permits a more even displacement of the eigenvalues with applied field.

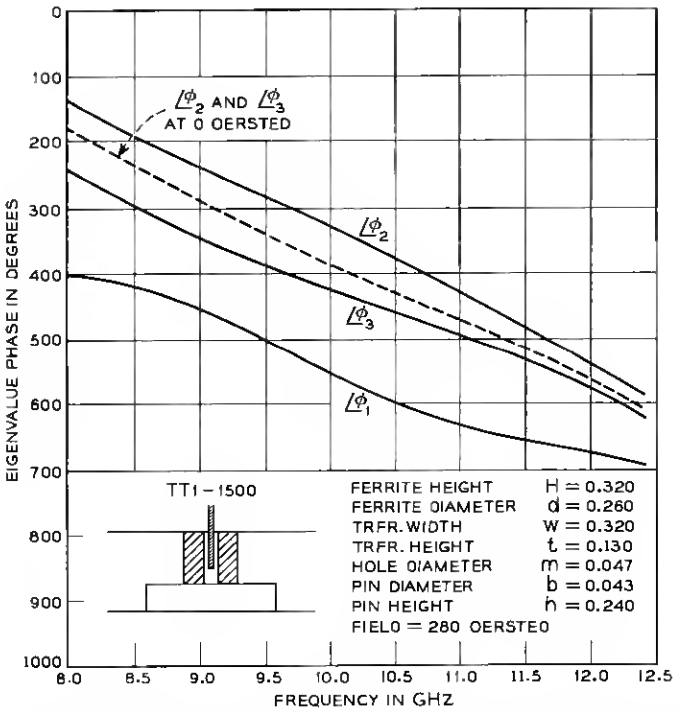

Fig. 22—The eigenvalue phase-frequency response of a junction with a transformer and pinned, full height ferrite. The eigenvalues have been linearized by the transformer in the vicinity of the $TM_{\pm 1,1,\delta}$ and $TM_{0,1,\delta}$ resonances. The field and pin have been adjusted for circulation.

of this relationship was not clearly understood before, and little was known about their modes of operation. The principal geometries considered here together with their modal responses are summarized in Table I.

The eigenvalue measuring set easily lends itself to direct circulator synthesis. It is much more powerful than the impedance plotting techniques previously used, and provides a quick-and-easy way of "arranging" for circulation. Only the phases of the eigenvalues need be considered when the losses are small. If losses are excessive or if a higher accuracy is required, then the eigenvalue magnitudes must also be taken into account. Since network analyzers are designed to measure both phase and amplitude, this does not present any measurement problem. The analysis of the results, however, is appreciably more difficult.

VI. ACKNOWLEDGMENTS

The author wishes to thank T. W. Mohr and J. J. Kostelnick for useful discussion, and K. P. Steinmetz for mechanical contributions. The advice, guidance, and contributions of C. E. Barnes throughout this work was invaluable and is greatly appreciated.

APPENDIX

From equation (8) and (3) respectively, the junction S parameters are given by,

$$\begin{aligned} S_{11} &= 1/3\{\phi_1 + \phi_2 + \phi_3\} \\ S_{31} &= 1/3\{\phi_1 + \phi_2 \exp(-j120^\circ) + \phi_3 \exp(+j120^\circ)\} \\ S_{21} &= 1/3\{\phi_1 + \phi_2 \exp(+j120^\circ) + \phi_3 \exp(-j120^\circ)\} \end{aligned} \tag{15}$$

where

$$\begin{aligned} S_{11} &= S_{22} = S_{33} \\ S_{31} &= S_{12} = S_{23} \\ S_{21} &= S_{13} = S_{32} \,. \end{aligned} \tag{16}$$

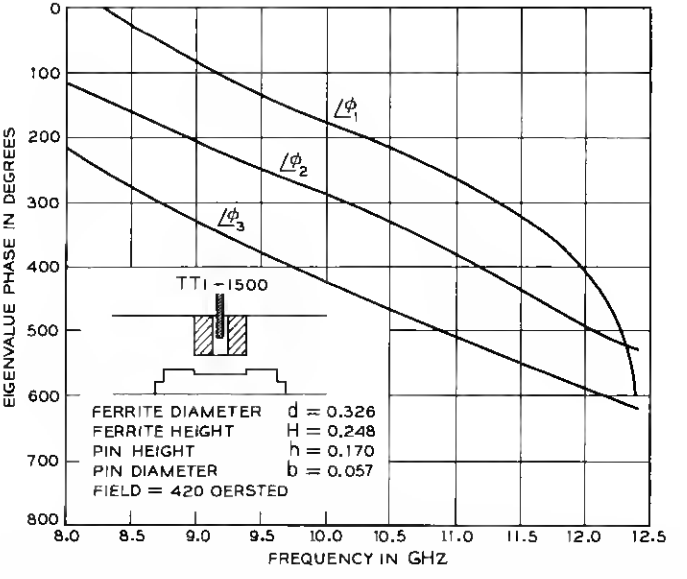

Fig. 23—The eigenvalue phase-frequency response of a very wideband circulator synthesized in a junction made from standard 0.900-inch wide and 0.400-inch high X-band waveguide.

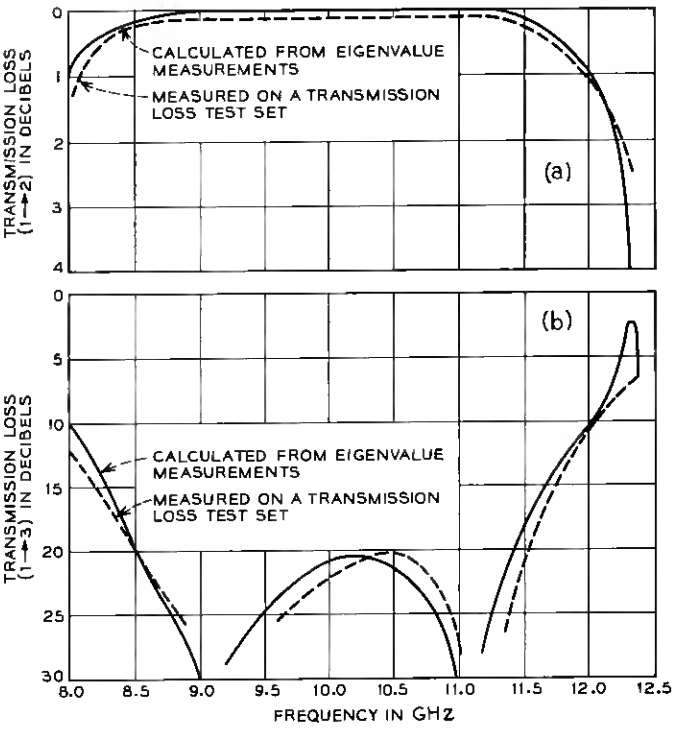

Fig. 24—Transmission loss from (a) ports 1 to 2 and (b) ports 1 to 3 for the junction in Fig. 23. The losses calculated from the eigenvalue phase are compared with those measured on a loss test set.

In more general terms, equation (1) is given by

$$S_{pq} = 1/3 \sum_{i=1}^{i=3} \alpha_i^{(pq)} \tag{17}$$

where S_{pq} is the ratio of the signal out of port p to the signal in at port q when only port q is excited; and $\alpha_i^{(pq)}$ is the ratio of the signal out of port p to the signal in at port q when the junction is excited by the ith eigen-excitation. When

(*i*) $p = q = 1$, then

$$S_{pq} = S_{11} \quad \text{and} \quad \alpha_i^{(11)} = \phi_i \, ,$$

(*ii*) $p = 3$ and $q = 1$, then

$$S_{pq} = S_{31} \quad \text{and} \quad \alpha_i^{(31)} = \phi_i \exp \{-j(i-1)120^\circ\}, \tag{18}$$

(*iii*) $p = 2$ and $q = 1$, then

$$S_{pq} = S_{21} \quad \text{and} \quad \alpha_i^{(21)} = \phi_i \exp\{+j(i-1)120^\circ\}.$$

We are interested in conditions in the junction when the S parameters are either zero or unity. Three possibilities exist, namely,

(*i*) $S_{11} = 1$ $S_{31} = 0$ $S_{21} = 0$ Total Reflection,
(*ii*) $S_{11} = 0$ $S_{31} = 1$ $S_{21} = 0$ Anticlockwise Circulation,
and (*iii*) $S_{11} = 0$ $S_{31} = 0$ $S_{21} = 1$ Clockwise Circulation.

S_{pq} is zero when the three components $\alpha_i^{(pq)}$ ($i = 1, 2, 3$) are phase displaced by 120 degrees from one another; and S_{pq} is unity when the same three components are in phase with each other. Suppose $\alpha_i^{(pq)}$ is measured for the three eigen-excitations by sampling the output signal on port p and the input signal on port q. Table II shows how these components must be displaced from one another for total reflection and for circulation. When the components measured are in phase with each other and $p \neq q$, the junction circulates. This provides a superior alternative to the 120 degrees displacement requirement normally aimed for in synthesis, since deviations from the ideal are so much more obvious. When the components measured are separated by 120 degrees from one another, the junction may be circulating or may be totally reflecting. One can determine which condition exists by noting the sequency of the measured phases. If circulation is indicated, a reversal of the biasing field will cause the measured components to coincide once more for the easy detection of variations.

TABLE I—A SUMMARY OF THE DIFFERENT RESONANT MODES EXCITED BY THE IN-PHASE AND ROTATING EIGEN-EXCITATIONS FOR DIFFERENT FERRITE GEOMETRIES

Ferrite Configuration	In-Phase Modes		Rotating Modes	
	Radial $TM_{0,n,0}$	Axial $TM_{0,n,z}$	Radial $TM_{\pm m,n,0}$	Axial $HE_{\pm m,n,z}$
Full Height	present		present	
Pinned and full height	present	present	present	present with large dia. pin only
Partial height	present		present	present
Pinned and partial height	present	present	present	present

TABLE II—PHASE REQUIREMENTS FOR CIRCULATION AND TOTAL REFLECTION WHEN THE INCIDENT AND REFLECTED WAVES ARE SAMPLED AT PORTS q AND p RESPECTIVELY

	Outgoing Signal Sampled at Port p Where		
	p=1	p=2	p=3
Ingoing Signal Sampled At Port q Where q=1.	Total Reflection When 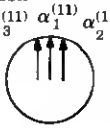	Total Reflection When 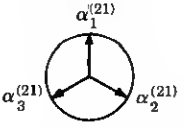	Total Reflection When 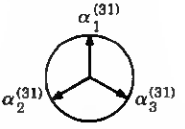
	Anticlockwise Circulation When 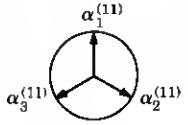	Anticlockwise Circulation When 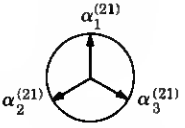	Anticlockwise Circulation When 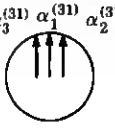
	Clockwise Circulation When 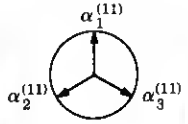	Clockwise Circulation When 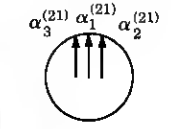	Clockwise Circulation When 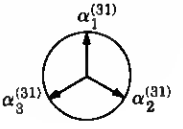

REFERENCES

1. Chait, H. N., and Curry, T. R., "Y Circulator," J. Appl. Phys., *30*, April 1959, p. 152.
2. Auld, B. A., "The Synthesis of Symmetrical Waveguide Circulators," IRE Trans. Microwave Theory and Techniques, *MTT-7*, No. 4 (April 1959, pp. 238–246.
3. Bosma, H., "On the Principle of Stripline Circulators," Proc. IEE, *109*, Part B Suppl., No. 21 (January 1962), pp. 137–146.
4. Fay, C. E., and Comstock, R. L., "Operation of the Ferrite Junction Circulator," IEEE Trans. Microwave Theory and Techniques, *MTT-13*, No .1 (January 1965), pp. 15–27.
5. Von Aulock, W. H., and Fay, C. E., *Linear Ferrite Devices for Microwave Application*, New York: Academic Press, 1968, p. 116.
6. Davies, J. B., "An Analysis of the m-Port Symmetrical H-Plane Waveguide Junction with Central Ferrite Post," IRE Trans. Microwave Theory and Techniques, *MTT-10*, No. 11 (November 1962), pp. 596–604.
7. Butterweck, H. J., "The Y Circulator," Arch. Elek. Ubertragung, *17*, No. 4 (December 1963), pp. 163–176.
8. Davies, J. B., "Theoretical Design of Wideband Waveguide Circulators," Electronics Letters, *1*, No. 3 (May 1965), pp. 60–61.
9. Parsonson, C. G., Longley, S. R., and Davies, J. B., "The Theoretical Design

of Broadband 3-Port Waveguide Circulators," IEEE Trans. Microwave Theory and Techniques, *MTT-16*, No. 4 (April 1968), pp. 256–258.
10. Castillo, J. B., Jr., and Davis, L. E., "Computer Aided Design of 3-Port Waveguide Junction Circulators," IEEE Trans. Microwave Theory and Techniques, *MTT-18*, No. 1 (January 1970), pp. 25–34.
11. Montgomery, C. G., Dickie, R. H., and Purcell, E. M., *Principles of Microwave Circuits*, New York: McGraw-Hill Book Co., Inc., 1948, p. 420.
12. Altman, J., *Microwave Circuits*, New York: D. Van Nostrand Co. Inc., 1964, p. 101.
13. Kurokawa, K., *An Introduction to the Theory of Microwave Circuits*, New York: Academic Press, 1969, p. 234.
14. Magalhaes, F. M., private communication.
15. Owen, B., and Barnes, C. E., "The Compact Turnstile Circulator," IEEE Trans. Microwave Theory and Techniques, *MTT-18*, No. 12 (December 1970), pp. 1096–1100.